Journal of Molecular Structure 1016 (2012) 126–133

Contents lists available at SciVerse ScienceDirect

Journal of Molecular Structure

journal homepage: www.elsevier.com/locate/molstruc

Synthesis and crystal structure analysis of substituted 2-(3-(hydroxymethyl)quinolin-2-yl)phenol derivatives

D. Rambabu [a,b], G. Rama Krishna [c], Srinivas Basavoju [d], M.V. Basaveswara Rao [e], C. Malla Reddy [c], Manojit Pal [a,*]

[a] Institute of Life Sciences, University of Hyderabad Campus, Hyderabad 500 046, Andhra Pradesh, India
[b] Department of Chemistry, K.L. University, Vaddeswaram, Guntur 522 502, Andhra Pradesh, India
[c] Department of Chemical Sciences, Indian Institute of Science Education and Research, Kolkata, West Bengal 741 252, India
[d] Department of Chemistry, National Institute of Technology (NIT), Warangal 506 004, Andhra Pradesh, India
[e] Department of Chemistry, Krishna University, Machilipatnam 521 001, Andhra Pradesh, India

ARTICLE INFO

Article history:
Received 24 December 2011
Received in revised form 19 February 2012
Accepted 21 February 2012
Available online 3 March 2012

Keywords:
2-(3-(Hydroxymethyl)quinolin-2-yl)phenol derivatives
Spectroscopic characterization
Single crystal X-ray diffraction
Supramolecular interactions
Conformational isomers
Helical structure

ABSTRACT

Two novel quinoline derivatives e.g. 2-(3-(hydroxymethyl)-7-methylquinolin-2-yl)phenol (**1**) and 2-(3-(hydroxymethyl)-6-methoxyquinolin-2-yl)phenol (**2**) were synthesized. These compounds were characterized by IR, ^{1}H NMR and mass spectroscopy. Thermal analyses (DSC and TGA) and PXRD patterns were collected for the supporting data. Finally the crystal structures were solved by single crystal X-ray diffraction data and the structures were analyzed in terms of supramolecular interactions. Compound **1** consists of two symmetry independent molecules in the asymmetric unit. These two molecules are conformational isomers (**A** and **B**) and form different hydrogen bonding in the crystal structure. The Hirshfeld surfaces and associated 2D fingerprint plots were analyzed to differentiate the two conformers (**A** and **B**). Compound **2** form a helical structure with O–H···O and O–H···N hydrogen bond synthons along the *c*-axis.

1. Introduction

The quinoline core is considered as a key pharmacophore responsible for the diverse pharmacological properties demonstrated by quinoline derivatives. Thus a wide variety of quinoline derivatives have been prepared and evaluated for their anticancer, antimycobacterial, antimicrobial, anticonvulsant, anti-inflammatory and cardiovascular activities [1]. Various quinoline alkaloids such as quinine, chloroquine, mefloquine and amodiaquine have been used as effective drugs for the treatment of malaria [2]. Development of resistance by plasmodia parasites has compromised the widespread use of these antimalarial drugs. Aryl substitution at C-2 position of the quinoline ring has been reported to induce good antibacterial activity [3,4]. These derivatives were found to be useful biological synthons and have attracted much attention in the development of new drugs [5,6]. In addition, they are ideally suitable for further modifications to obtain more efficacious antibacterial and antituberculosis agents.

Recently, Sumesh et al., reported the synthesis and evaluation of 1,3-oxazolo[4,5-c]quinoline derivatives which showed antibacterial and antituberculosis activities when tested *in vitro*. Their screening results revealed that all the compounds showed moderate to very good activity against pathogenic strains such as *Escherichia coli* (ATTC-25922), *Staphylococcus aureus* (ATTC-25923), *Pseudomonas aeruginosa* (ATCC-27853), *Klebsiella pneumoniae* and Mycobacterium tuberculosis H37Rv [7]. Kategaonkar et al., reported the synthesis and biological evaluation of 2-chloro-3-((4-phenyl-1*H*-1,2,3-triazol-1-yl)methyl)quinoline derivatives *via* click chemistry approach [8]. These molecules were evaluated *in vitro* for their antifungal and antibacterial activities. Most of these compounds displayed significant activities against all the tested strains. Quinoline derivatives, protoberbines and 8-oxoberbines are known to possess biological properties such as antineoplastic activity [9]. The potent antitumor agents e.g. Dynamicin A and Virantmycin are important natural products containing the quinoline core [10]. Ahmed et al. synthesized the naturally occurring quinolone alkaloids and their inhibitory properties (antiproliferative activity) were evaluated against CEM-GFP cells [11]. These results have attracted the attention to synthesize the quinoline derivatives.

Recently, (2-chloro-6-methoxyquinolin-3-yl)methanol, **8** (Scheme 1) has been reported to exhibit significant cytotoxic activities when tested *in vitro* (IC_{50} = 42.5 and 47.4 μg/mL on HeLa

* Corresponding author. Tel.: +91 40 66571633.
E-mail address: manojitpal@rediffmail.com (M. Pal).

0022-2860/$ - see front matter © 2012 Elsevier B.V. All rights reserved.
doi:10.1016/j.molstruc.2012.02.054

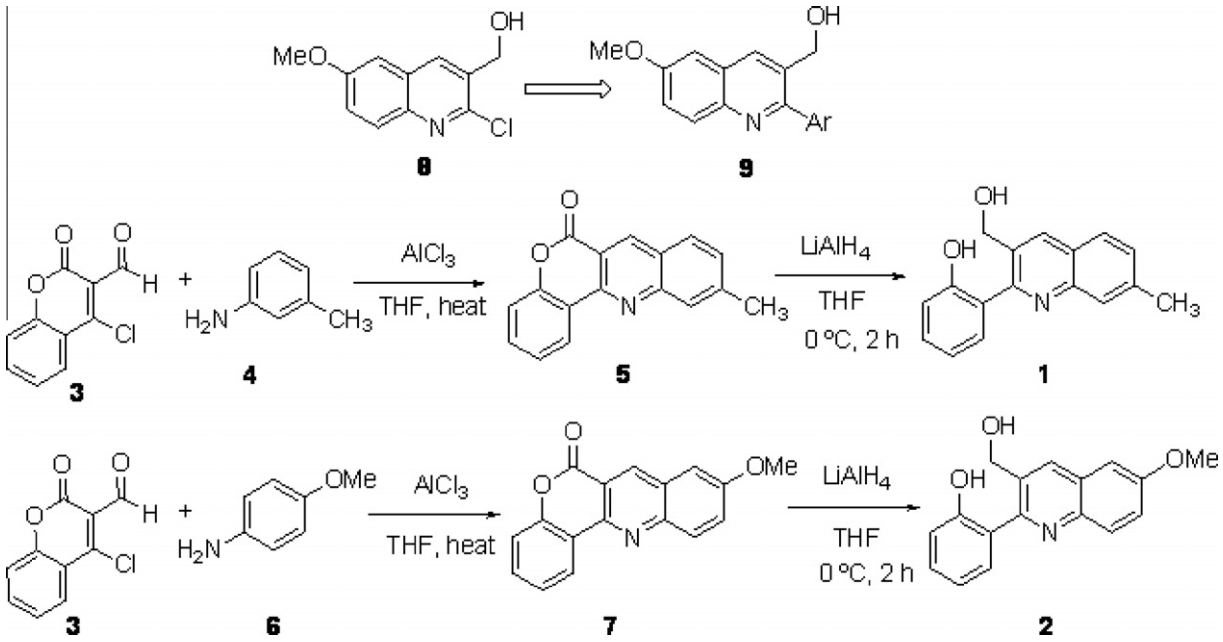

Scheme 1. Synthesis of compounds **1** and **2**.

and Vero cells, respectively) [12]. Due to our continuing interest in the identification of quinoline derivatives as cytotoxic agents we became interested to prepare the derivatives of compound **8** such as compound **9** (Scheme 1) for *in vitro* pharmacological evaluation. Herein, we report the synthesis and characterization of 2-(3-(hydroxymethyl)-7-methylquinolin-2-yl)phenol (**1**) and 2-(3-(hydroxymethyl)-6-methoxyquinolin-2-yl)phenol (**2**) along with their single crystal X-ray analysis data.

2. Experimental

2.1. Chemicals

m-Toluidine (**4**) (purity > 99.8%) and *p*-anisidine (**6**) (purity > 99.8%) were purchased from Aldrich Co. Ltd. 4-Chloro-3-formylcoumarin (**3**) (purity > 99.8%) was synthesized according to the literature procedures [13]. All the commercially available reagents (purity > 99%) were used without further purification. The solvent THF was dried over sodium-benzophenone before use.

2.2. General methods

All reactions were carried out under nitrogen atmosphere. Melting points were determined on a Büchi B-540 melting point apparatus and are uncorrected. All compounds were routinely checked by TLC and ^{1}H NMR. TLC was performed on aluminum-backed silica gel plates (Merck DC, Alufolien Kieselgel 60 F254) with spots visualized by UV light.

2.3. ^{1}H and ^{13}C NMR spectroscopy

^{1}H and ^{13}C NMR spectra were determined in $CDCl_3$, DMSO-d_6 and TFA solutions using 400 and 100 MHz spectrometers, respectively. Proton chemical shifts (δ) are relative to tetramethylsilane (TMS, $\delta = 0.0$) as internal standard and expressed in parts per million. Spin multiplicities are given as s (singlet), d (doublet), t (triplet), and m (multiplet) as well as *b* (broad). Coupling constants (*J*) are given in hertz.

2.4. Infrared spectroscopy

Jasco FT–IR 4200 (Easton, Maryland) type-A Fourier transform infrared spectrophotometer was used to record the IR spectra of the samples (sample concentration is 2 mg in 20 mg of KBr). The spectra were recorded over the range of 4000–600 cm^{-1}. Data were analyzed using spectrum version 2 software (JASCO, Easton, Maryland, USA).

Table 1
Salient crystallographic data and structure refinement parameters of compounds 1 and 2.

	1	**2**
Empirical formula	$C_{17}H_{15}NO_2$	$C_{17}H_{15}NO_3$
Formula weight	265.30	281.30
Crystal system	Monoclinic	Tetragonal
Space group	$P2_1/c$	I-4
T/K	100(2)	296(2)
a/Å	16.8103(10)	17.4497(7)
b/Å	12.9741(8)	17.4497(7)
c/Å	12.9263(8)	8.9605(4)
α/°	90.00	90.00
β/°	99.911(4)	90.00
γ/°	90.00	90.00
Z	8	8
V/Å^3	2777.1(3)	2728.4(3)
D_{calc}/g/cm^3	1.269	1.370
$F(000)$	1120.0	1184
μ/mm^{-1}	0.083	0.094
θ/°	2.36–26.99	1.65–26.99
Index ranges	$-20 \le h \le 20$	$-22 \le h \le 22$
	$-15 \le k \le 15$	$-18 \le k \le 22$
	$-15 \le l \le 15$	$-11 \le l \le 11$
N-total	59,742	9762
N-independent	5188	1593
N-observed	3748	1515
Parameters	367	198
R_{int}	0.110	0.050
R_1 ($I > 2\sigma(I)$)	0.0490	0.0330
wR_2 (all data)	0.1443	0.0904
GOF	1.037	1.052
CCDC	826,485	826,484

Table 2
Geometrical Parameters of Hydrogen bonds in 1 and 2.

Compound	D–H···A [a]	D···A (Å)	H···A (Å)	D–H···A (°)	Symmetry code
1	O(1)–H(1)···O(2)	2.713(2)	1.90	170	$-x, 2-y, 1-z$
	O(2)–H(2)···N(1)	2.755(2)	1.94	170	$-x, 1/2+y, 3/2-z$
	O(3)–H(3A)···O(4)	2.759(2)	1.94	175	$1-x, 1/2+y, 1/2-z$
	O(4)–H(4A)···N(2)	2.716(2)	1.91	169	$x, 1/2-y, 1/2+z$
	Intra C(16)–H(16A)···O(1)	2.982(3)	2.52	109	–
	Intra C(20)–H(20)···O(4)	2.761(2)	2.42	102	–
2	O(1)–H(1)···O(2)	2.671(2)	1.77(3)	173(3)	$-y, x, 1-z$
	O(2)–H(2)···N(1)	2.758(2)	1.83(4)	168(4)	$1/2-y, -1/2+x, 1/2-z$
	C(3)–H(3)···O(2)	2.778(2)	2.43	102	–
	C(17)–H(17C)···O(1)	3.400(3)	2.58	144	$y, -x, -z$

[a] All of the C–H and O–H distances are neutron normalized to 1.083 and 0.983 Å.

2.5. Differential Scanning Calorimetry (DSC)

Thermal analyses of these samples were performed on a Thermal Advantage DSC Q2000 V9.8 Build 296 (TA Instrument, USA) module which was calibrated for temperature and cell constants using indium and sapphire. The instrument was equipped with refrigerator cooling system (RCS). The crystals (3–5 mg) were crimped in aluminum pans (non-hermetic) (30 μL) scanned at a heating rate of 10 °C/min in the range 30–300 °C under a dry nitrogen atmosphere (flow rate 50 mL/min). The data were collected by TA Instruments Universal Analysis 2000 V4.3A software.

2.6. Thermogravimetric Analysis (TGA)

Thermal analyses of these samples were carried out by TA Instrument (USA) TGA Q5000 module with refrigerator cooling system (RCS). The crystals (5–10 mg) were placed in aluminum crucibles (30 μL) under a dry nitrogen atmosphere (flow rate is 25 mL/min). The data were collected by TI Universal Analysis software.

2.7. Powder X-ray Diffraction (PXRD)

PXRD patterns were collected on a Rigaku D/MAX 2200 (The Woodlands, Texas) powder diffractometer with a Cu Kα radiation (1.54056 Å). The tube voltage and amperage were set at 50 kV and 34 mA respectively. The divergence slit and antiscattering slit settings were variable for the illumination on the 20 mm sample size. Each sample was scanned 3° and 45° in 2θ with a step size of 0.02°. The instrument had previously been calibrated using a silicon standard.

2.8. Single crystal X-ray diffraction

The single-crystal X-ray diffraction data of the crystals were collected on a Bruker Kappa APEX-II CCD DUO diffractometer at 296(2) K using graphite-monochromated Mo Kα radiation (λ = 0.71073 Å). No absorption correction was applied. The lattice parameters were determined from least-squares analysis, and reflection data were integrated using the program SHELXTL [14]. The crystal structures were solved by direct methods using SHELXS-97 and refined by full-matrix least-squares refinement on F^2 with anisotropic displacement parameters for non-H atoms using SHELXL-97 [15]. The O−H hydrogens were located from difference Fourier maps. Aromatic and aliphatic C−H hydrogens were generated by the riding model in idealized geometries. The software used to prepare material for publication was Mercury 2.3 (Build RC4), ORTEP-3 and X-Seed [16]. Table 1 gives the pertinent crystallographic data, and Table 2 gives hydrogen bond parameters.

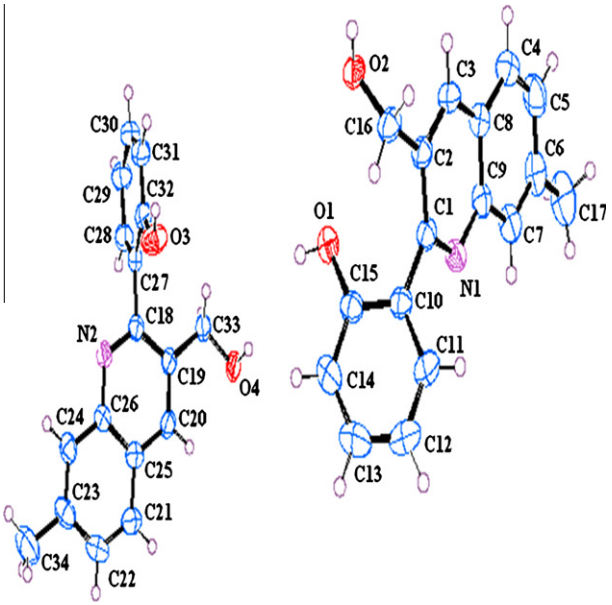

Fig. 1. ORTEP representation of conformers **A** and **B** of compound **1**. Thermal ellipsoids are drawn at 50% probability level.

2.9. Synthesis

The target compound **1** was prepared following a two-step procedure, the reaction of 4-chloro-3-formylcoumarin (**3**) with *m*-toluidine (**4**) being the key step (Scheme 1). Thus 9-methyl-6*H*-chromeno[4,3-*b*]quinolin-6-one (**5**) was prepared by $AlCl_3$-mediated condensation reaction of **3** with **4** according to a known procedure [17]. A similar procedure was used for the preparation of compound **7**, by using **3** and **6**.

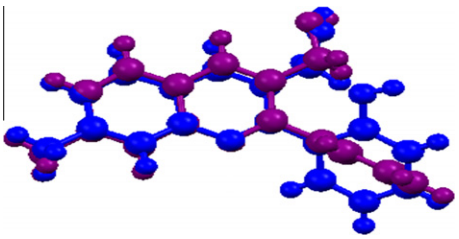

Fig. 2. An overlay diagram of conformers **A** (blue) and **B** (purple) of the two molecules of asymmetric unit of compound **1**. It is visible that the two phenyl rings are not in coplanar with the quinoline moiety. (For interpretation of the references to colour in this figure legend, the reader is referred to the web version of this article.)

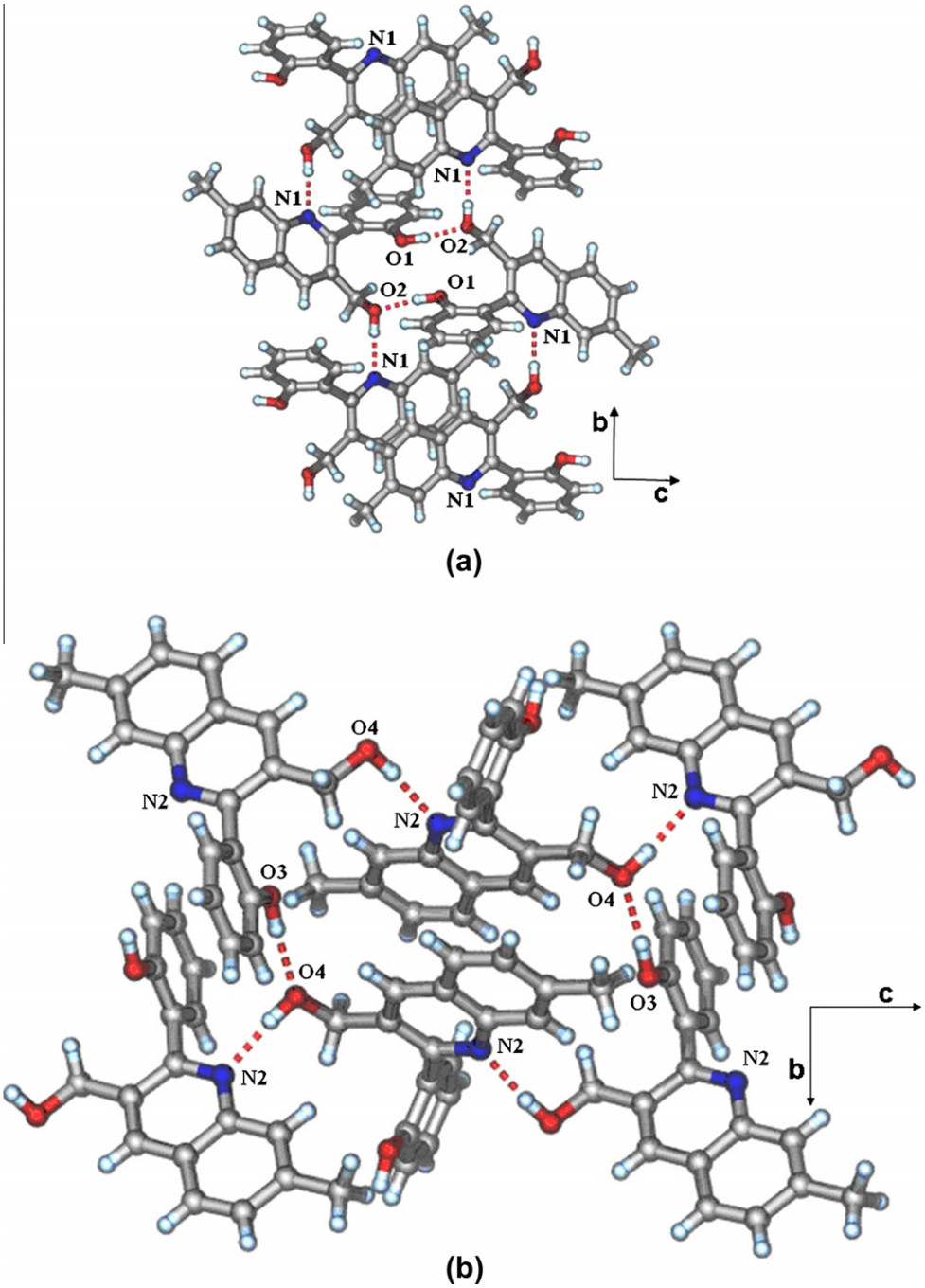

Fig. 3. (a and b) Different hydrogen bonding patterns in two symmetry independent molecules (conformers **A** and **B**) of asymmetric unit in compound **1**.

Spectral data for compound **5**, white solid; yield (90%); R_f = 0.60 (30% EtOAc-*n*-Hexane); m.p. 228–230 °C; ^{1}H NMR (400 MHz, $CDCl_3$): δ 9.12 (s, 1H), 8.77 (dd, J = 8.0 and 1.6 Hz, 1H), 8.14 (d, J = 8.4 Hz, 1H), 7.76–7.74 (m, 2H), 7.58–7.56 (m, 1H), 7.45–7.38 (m, 2H), 2.59 (s, 3H); ^{13}C NMR (100 MHz, DMSO-d_6): δ 160.9, 152.8, 150.8, 149.6, 145.1, 140.9, 132.9, 130.3, 129.9, 128.0, 125.8, 125.3, 124.9, 119.8, 117.7, 115.6, 22.3; MS (ES mass): m/z 262.3 (M+1, 100%); IR (KBr) υ_{max} (cm^{-1}): 3449, 3055, 2923, 1735, 1599, 1497, 1462, 1378, 1310, 1188, 900, 826, 754.

Spectral data for compound **7**, white solid; yield (91%); R_f = 0.71 (20% EtOAc-*n*-Hexane); mp 236–238 °C; ^{1}H NMR (400 MHz, $CDCl_3$): δ 9.1 (s, 1H), 8.76 (dd, J = 10 and 1.6 Hz, 1H), 8.14 (d, J = 9.2 Hz, 1H), 7.60–7.55 (m, 2H), 7.45–7.39 (m, 2H), 7.23 (d, J = 2.8 Hz, 1H), 3.99 (s, 3H); ^{13}C NMR (100 MHz, TFA): δ 159.6, 153.8, 151.6, 147.6, 142.2, 138.9, 134.7, 134.6, 127.2, 124.8, 124.0, 122.1, 121.8, 118.9, 105.9, 105.6, 58.8; MS (ES mass): m/z 278.3 (M+1, 10%); IR (KBr) υ_{max} (cm^{-1}): 3100, 2990, 2836, 1737, 1601, 1496, 1384, 1237, 835, 749.

2.10. Preparation of 2-(3-(hydroxymethyl)-7-methylquinolin-2-yl)phenol (1)

A solution of 9-methyl-6*H*-chromeno[4,3-*b*]quinolin-6-one, **5** (200 mg, 1.0 mmol) in dry THF (15 mL) was cooled to 0 °C and $LiAlH_4$ (40 mg, 1.2 mmol) was added portion wise with stirring under a nitrogen atmosphere. The duration of addition was 15 min. The mixture was then warmed to room temperature and stirring continued. After completion of the reaction the mixture was quenched with water (15 mL) and extracted with ethyl acetate (2 × 100 mL). The organic layers were collected, combined, washed

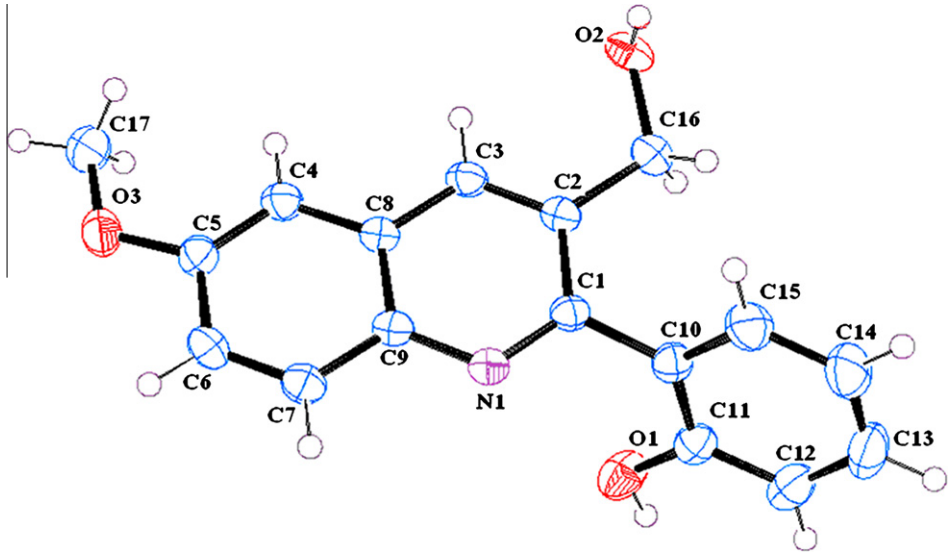

Fig. 4. ORTEP representation of compound **2**. Thermal ellipsoids are drawn at 50% probability level.

with cold water (2 × 50 mL), dried over anhydrous Na_2SO_4, filtered and concentrated under vacuum. The residue was purified by flash chromatography using 1:1 *n*-hexane/ethyl acetate to give the required product **1**. The pure compound **1** was crystallized from acetonitrile to give needle shaped crystals.

Spectral data for compound **1**, white solid; yield (150 mg, 74%); R_f = 0.60 (30% EtOAc-*n*-Hexane); m.p. 185–187 °C; ^{1}H NMR (400 MHz, DMSO-d_6): δ 10.02 (s, 1H), 8.30 (s, 1H), 7.91–7.84 (m, 1H), 7.40–7.34 (m, 1H), 7.32–7.20 (m, 3H), 6.94–6.87 (m, 2H), 5.25 (t, J = 5.6 Hz, 1H), 4.47 (d, J = 5.2, 2H), 3.88 (s, 3H); ^{13}C NMR (100 MHz, DMSO-d_6): δ 157.9, 157.2, 144.7, 138.3, 132.5, 131.2, 130.4, 129.8, 127.6, 127.5, 127.1, 126.7, 121.3, 119.1, 118.2, 62.9, 21.30. MS (ES mass): m/z 266.1 (M+1, 10%); IR (KBr) υ_{max} (cm^{-1}): 3120, 3079, 2941, 2470, 2028, 1796, 1493, 1435, 1025, 1068, 740, 637; HPLC: 99.5%.

2.11. Preparation of 2-(3-(hydroxymethyl)-6-methoxyquinolin-2-yl)phenol (2)

A similar procedure as described above was followed for the preparation of **2**. The pure compound **2** was crystallized from acetonitrile to give needle shaped crystals.

Spectral data for compound **2**, white solid; yield (145 mg, 65%); R_f = 0.60 (30% EtOAc-n-Hexane); m.p. 230–232 °C; ^{1}H NMR (400 MHz, DMSO-d_6): δ 10.02 (s, 1H), 8.30 (s, 1H), 7.85 (d, J = 8.8, 1H), 7.36 (d, J = 9.2, 1H), 7.27–7.20 (m, 3H), 6.93–6.87 (m, 2H), 5.25 (t, J = 5.6, 1H), 4.47 (d, J = 5.2, 2H), 3.88 (s, 3H); ^{13}C NMR (100 MHz, DMSO-d_6): δ 154.8, 141.9, 135.4, 131.6, 130.3, 129.8, 129.5128.6, 128.1, 126.6, 121.2, 118.9, 115.6, 105.4, 59.9, 55.3, 29.0; MS (ES mass): m/z 282.1 (M+1, 10%); IR (KBr) υ_{max} (cm^{-1}): 3074, 2994, 2754, 1621, 1596, 1496, 1456, 1227, 1051, 926, 756; HPLC: 99.9%.

2.12. Preliminary characterization

The shapes of the crystals of the compounds **1** and **2** were observed under the LEICA DFC295 polarizing microscope.

3. Results and discussion

3.1. Infrared spectroscopy analysis

IR spectra of the compounds **1** and **2** are given in supplementary material (see Fig. S3 and S4). A broad peak at 3151 cm^{-1} shows that the presence of –OH group in the molecule that is involved in hydrogen bonding and this was confirmed by single crystal X-ray structure analysis. The disappearance of strong absorption at 1735 and 1737 cm^{-1} corresponding to the lactone carbonyl group of compounds **5** and **7** respectively, showed that they were completely reduced to give compound **1** and **2** respectively. The peaks in compound **1** appeared at 2941 and 2804 cm^{-1} were due to the –CH_3 and –CH_2 groups. The stretching frequencies at 2994 and 2836 cm^{-1} were due to the –CH_3 and –CH_2 groups respectively in compound **2**. A broad peak at 3100 cm^{-1} was due to the –OH group present in compound **2** and involved in strong hydrogen bonding. This was later confirmed by single crystal X-ray structure. A peak at 1456 cm^{-1} accounts for the –OCH_3 linkage in compound **2**.

3.2. DSC and TGA analyses

DSC and TGA thermograms (Supplementary material Fig. S23–S26) show the thermal behavior of the compounds **1** and **2**. DSC thermogram of compound **1** shows that a sharp endothermic peak at 175.82 °C (melting point: 185–187 °C) attributed to its melting point and no endothermic peak below the melting point shows that there was no inclusion of solvent in the crystal. In compound **2**, an endothermic peak at 203.99 °C (melting point: 230–232 °C) corresponds to its melting range and a small endotherm at 198.6 °C shows a phase transition. TGA shows that there was no weight loss in the two compounds and found that they are anhydrous in nature. It was finally confirmed by single crystal X-ray diffraction.

3.3. PXRD analysis

The PXRD patterns of compounds **1** and **2** were given in Supplementary Information (Fig. S19–S22).

3.4. Crystal structure analysis

With regard to structural analysis of compound **1**, it crystallizes in the centrosymmetric monoclinic $P2_1/c$ space group with two symmetry independent molecules in the asymmetric unit (Z' = 2) (Fig. 1). The two *o*-hydroxyphenyl rings of the molecules in the asymmetric unit are not coplanar with quinoline moieties of the two molecules. The torsion angles of the phenyl ring and quinoline

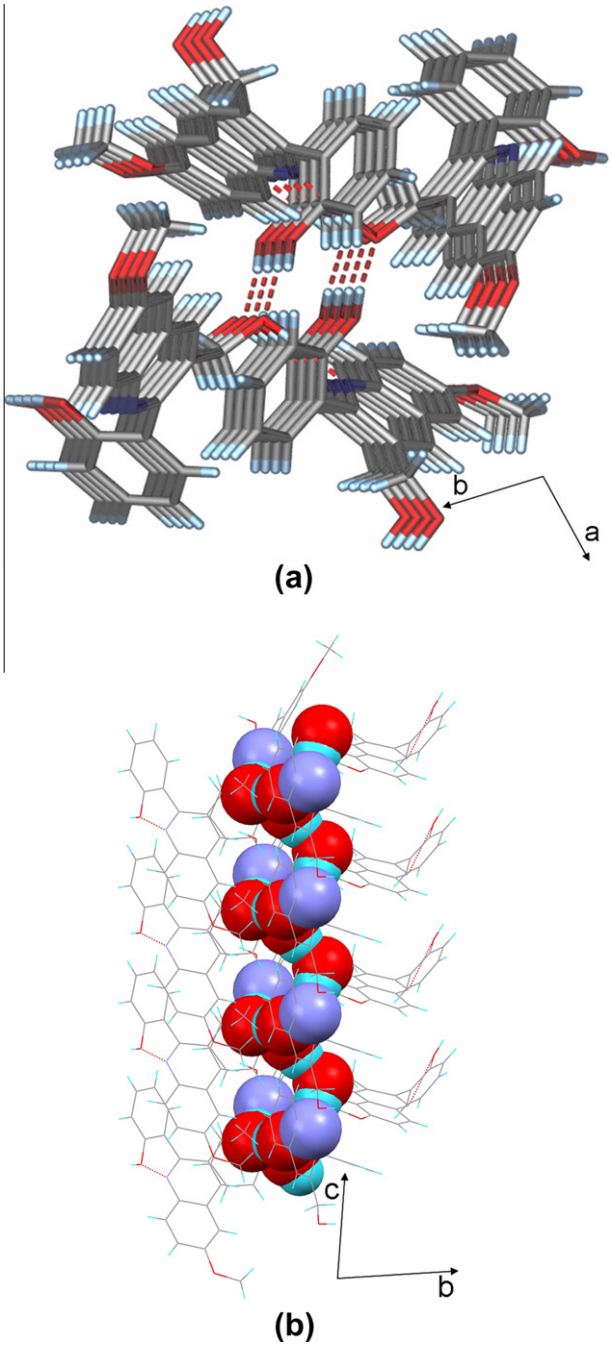

Fig. 5. A helical structure with O–H···O and O–H···N hydrogen bonds in compound **2**. (a) viewdown *c*-axis; (b) spacefill model to show the helical structure with O–H···O and O–H···N interactions (viewdown *a*-axis).

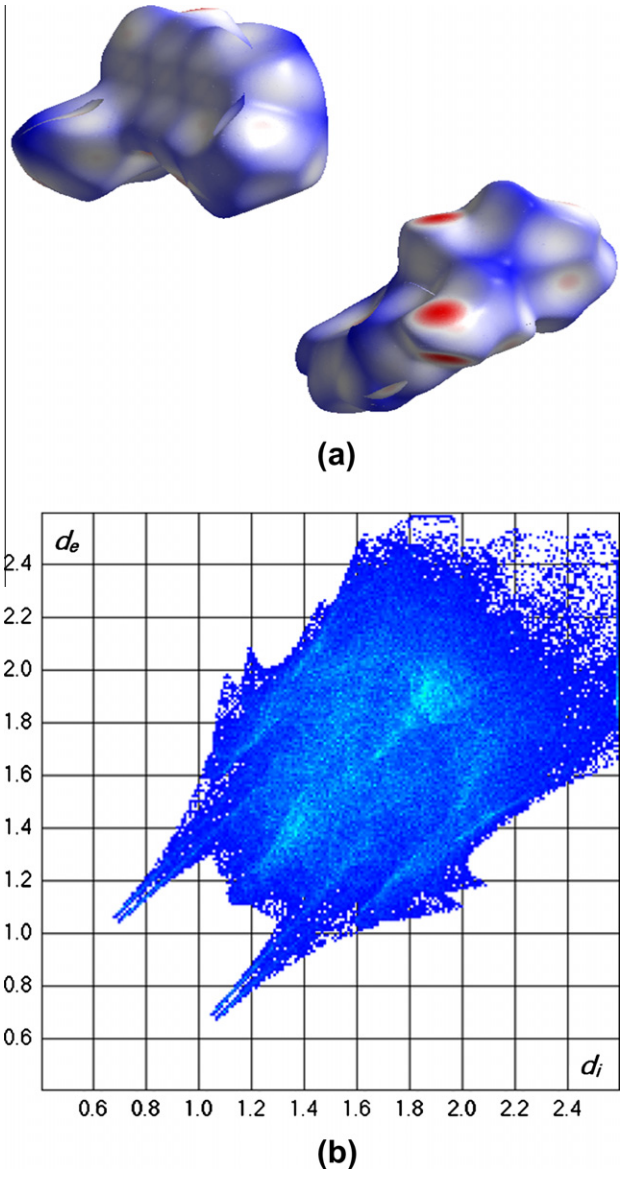

Fig. 6. Shows (a) Hirshfeld surface and (b) 2D fingerprint plot of compound-**1**.

moieties are −124.66° (N1–C1–C10–C15) and 99.49° (N2–C18–C27–C28). Interestingly, the two molecules in the asymmetric unit of compound **1** form different hydrogen bonding patterns in the crystal structure. These two molecules of compound **1** are conformationally different (Fig. 2). The inversion related molecules of conformer-**A**, form a supramolecular dimer with robust O–H···O synhons (d = 1.90 Å, θ = 170°) with the phenolic –OH and –CH_2OH groups. The free hydrogens of the phenolic O–H and –CH_2OH groups of this dimer interact with screw related molecules via O–H···N hydrogen bonds (d = 1.94 Å, θ = 170°) to form a supermolecule. These interactions propagate in 2D and form a corrugated layered structure (Fig. 3a). Two pairs of inversion related molecules of the conformer-**B** interact with each other via H_2C–OH···N (d = 1.91 Å, θ = 169°) and Ph–OH···OH–CH_2 (d = 1.94 Å, θ = 175°) hydrogen bonds to form a tetramer. These interactions propagate in 1D and 2D to form a corrugated layered structure (Fig. 3b). The corrugated layers of the two conformers arranged alternatively along the (100) plane. Missing the dimer in conformer-**B** indicate that the two molecules in the asymmetric unit in compound-**1** are conformational isomers.

Compound **2** crystallizes in the tetragonal *I*-4 space group with one molecule in the asymmetric unit (Fig. 4). The *o*-hydroxyphenyl moiety is not in coplanar with the quinoline moiety. The torsion angle between the *o*-hydroxyphenyl and quinoline moieties (N1–C1–C10–C15) is −112.69°. The molecules in the crystal structure form helical structure with the phenolic –OH groups of one molecule, –CH_2–OH group of another molecule and quinoline nitrogen of the another molecule via O–H···O (d = 1.77(3) Å, θ = 173(3)°) and O–H···N (d = 1.83(4) Å, θ = 168(4)°) synthons along the *c*-axis (Fig. 5a and b). These interactions are extended along *a* and *b* axes and form a helical structures. Notably, the –OCH_3 group of compound **2** was not involved in any hydrogen bonding.

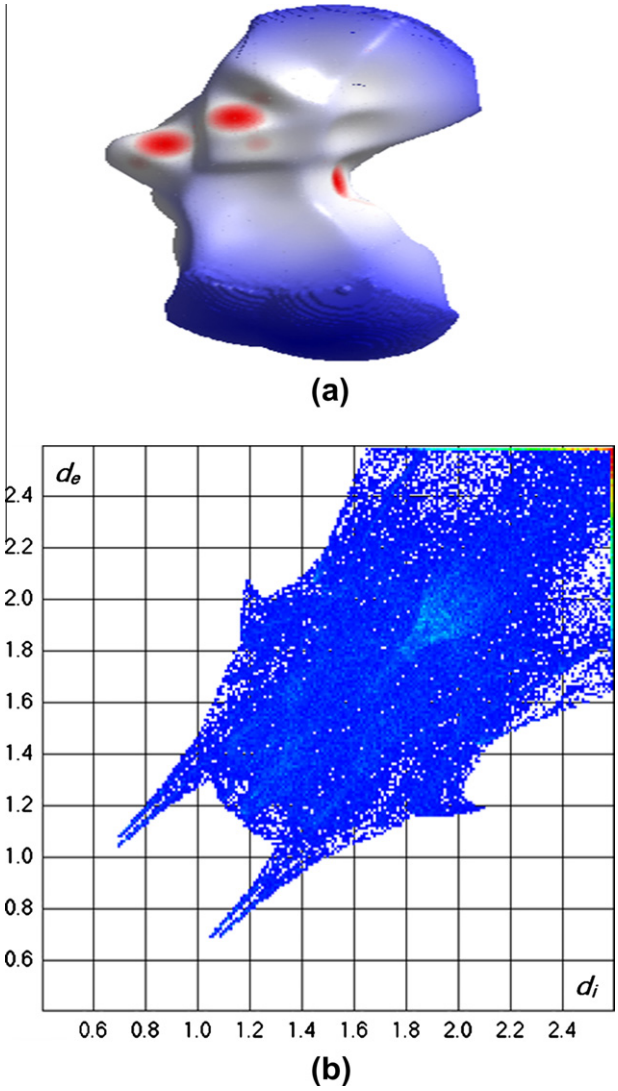

Fig. 7. Shows (a) Hirshfeld surface and (b) finger print plot of conformer-**A** of compound-**1**.

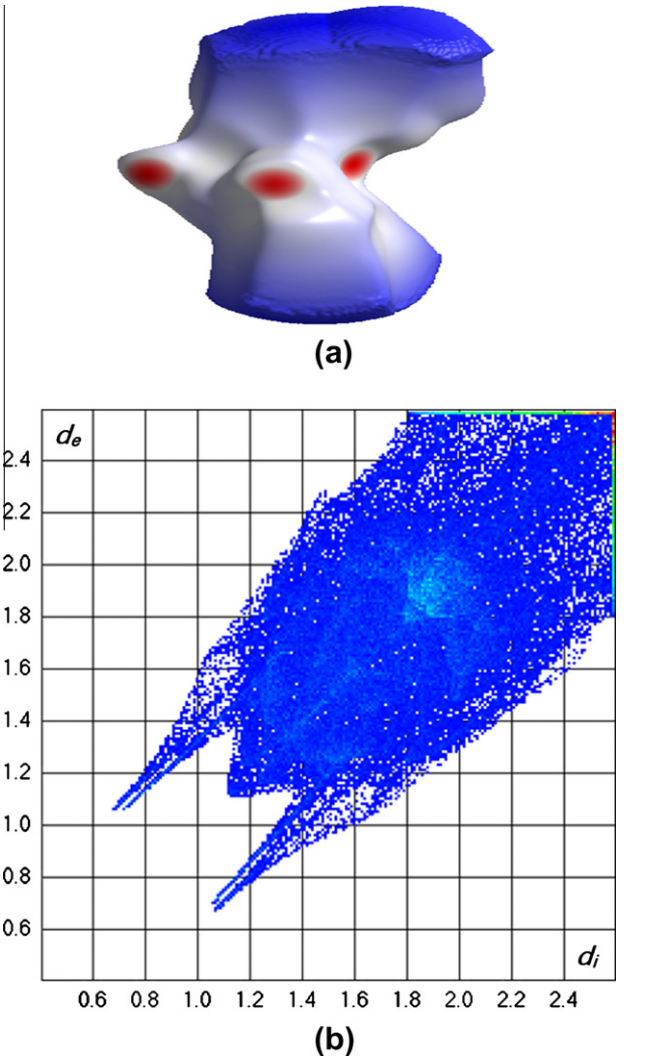

Fig. 8. Shows (a) Hirshfeld surface and (b) finger print picture of conformer-**B** of compound-**1**.

3.5. CSD analysis

Cambridge analysis database (ConQuest version 5.27, Nov 2005, number of hits 3,55,064) search for 2-phenylquinoline moiety was performed. Good-quality structures containing ordered, error-free, and nonpolymeric organic compounds with 3D coordinates and having $R < 5\%$ were chosen for the analysis. Only 5 molecules were found the in the analysis. Among 5 molecules two molecules (refcodes: MENBAJ VIHGOI) are N-oxides. It is observed from the search that there is no more than one same molecule in the asymmetric unit, like in compound **1**.

3.6. Hirshfeld surface analysis

It is difficult to understand the intermolecular interactions in polymorphic structures by visualizing the three dimensional structures. However, graphical tools based on the Hirshfeld surface and the two dimensional (2D) fingerprint plots [18] offered considerable promise for exploring packing patterns and intermolecular interactions in molecular crystals. As emphasized in the literature the size and shape of a Hirshfeld surface reflects the interaction between different atoms and intermolecular contacts in a crystal, and hence the surfaces essentially reflect different intermolecular interactions. A challenging task is to successfully differentiate the conformational polymorphism by analyzing the crystal structures. But the Hirshfeld surface analysis made easy to differentiate the polymorphic forms and conformational polymorphism. Since the Hirshfeld surfaces are directly depend on the molecular environment, these are unique in the given crystal structure and they depend on the number of crystallographically independent molecules present in the asymmetric unit. Here we have applied the Hirshfeld surface and 2D fingerprint plots to analyze the conformers **A** and **B** of compound-**1**.

The 2D fingerprint plots of compound-**1** were derived from the Hirshfeld surface by plotting the fraction of points on the surface as a function of the pair (di, de). Each point on the standard 2D graph represents a bin formed by discrete intervals of di and de (0.01×0.01 Å), and the points are colored as a function of the fraction of surface points in that bin, with a range from blue (relatively few points) through green (moderate fraction). The Hirshfeld surfaces and 2D fingerprint plots are given in Figs. 6–8. It is obvious from this analysis that the two conformers-**A** and **B** of compound-**1** are completely different and exhibit the conformational isomerism. Inspection of the fingerprint plots in Figs. 7b and 8b highlights the major differences between the two conformers. The conformer-**A** features the diffuse region of the blue points

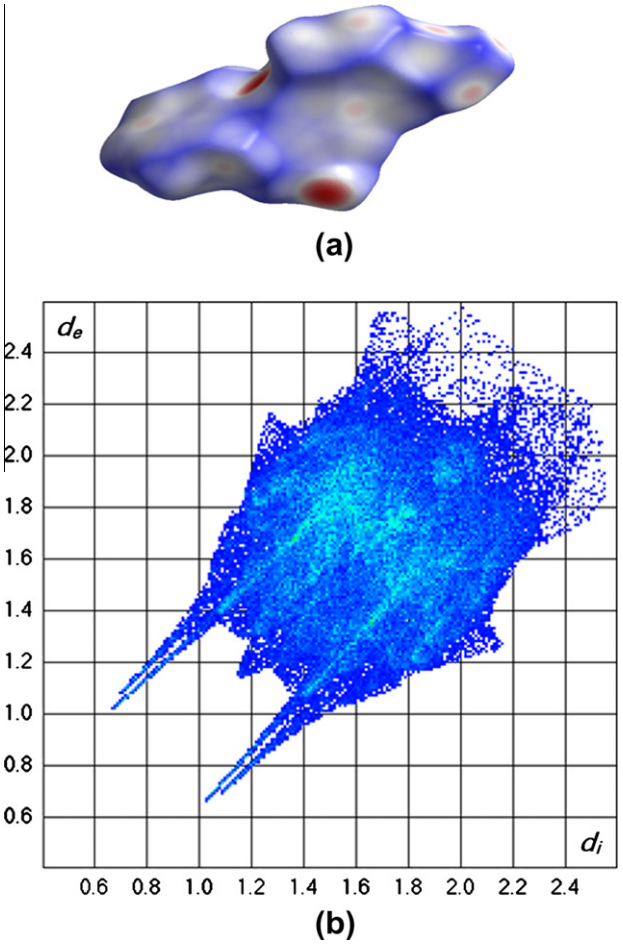

Fig. 9. Shows (a) Hirshfeld surface and (b) fingerprint picture of compound-**2**.

between the hydrogen bond spikes, while this feature is sharpened in the fingerprint plot of conformer-**B**. The Hirshfeld surface and fingerprint plots of compound-**2** are given in Fig. 9a and b.

4. Conclusions

The compounds **1** and **2** were synthesized and characterized by spectral data (^{1}H NMR, IR and Mass). The structures of the compounds **1** and **2** were finally determined by single crystal X-ray diffraction data. Due to the torsion angles of the phenyl ring and quinoline moieties, the compound **1** exhibits conformational isomerism and the two conformers (**A** and **B**) form different hydrogen bond synthons. The Hirshfeld surface analysis associated with 2D finger plots were carried out on the two conformers (**A** and **B**) of compound **1**. It is evident from this analysis that the two conformers are completely different and they form different hydrogen bonds in the crystal structure. The compound **2** forms helical structure in the crystal structures with O–H···O and O–H···N hydrogen bond synthons. The biological evaluation of these two compounds is in progress in our laboratory. This work contributes the synthesis of novel quinoline derivates and the use of Hirshfeld surface analysis to identify the conformational isomers.

Acknowledgements

DRB thanks Prof. Javed Iqbal, Director of ILS for his continuous support and encouragements. CMR thanks the DST, New Delhi, India for funding. GRK thanks IISER, Kolkata, India for a Senior Research Fellowship.

Appendix A. Supplementary material

Spectral data (IR, MASS, NMR, HPLC, PXRD, DSC and TGA) of the compounds **1** and **2** are available in the supporting information in .pdf format. Crystallographic information files (.cif) for the compounds **1** and **2** are available in the electronic format. Supplementary data associated with this article can be found, in the online version, at doi:10.1016/j.molstruc.2012.02.054.

References

[1] S. Kumar, S. Bawa, H. Gupta, Mini Rev. Med. Chem. 9 (2009) 1648;
A. Robert, B. Meunier, Chem. Soc. Rev. 27 (1998) 273.
[2] M.E. Jason, W.C. Robert, C. Mark, G.C. Gary, H.H. Peter, A.J. Brian, A. MacLeod, M. Rose, M.L. Georgina, M. Elena, M. Fraser, R. Michael, R. Inmaculada, G.N.R. Michael, S. Bindi, L.T. Kwei, W. Brian, Bioorg. Med. Chem. Lett. 50 (2006) 5748.
[3] J. Nilsson, E.Ø. Nielsen, T. Liljefors, M. Nielsen, O. Sterner, Bioorg. Med. Chem. Lett. 18 (2008) 5713.
[4] M. Simeon, N. John, L. Georgia, K. Eleni, G. Vasiliki, T. Dimitrios, N. Pavlos, Int. J. Antimicrob. Agents 29 (2007) 738.
[5] N. Kaila, K. Janz, S. DeBernardo, P.W. Bedard, R.T. Camphausen, S. Tam, D.H.H. Tsao, J.C. Keith Jr., C.N. Nutter, A. Shilling, R.Y. Sciame, Q. Wang, J. Med. Chem. 50 (2007) 21.
[6] K.E. Andersen, B.F. Lundt, A.S. Jørgensen, C. Braestrup, Eur. J. Med. Chem. 31 (1996) 417.
[7] S. Eswaran, A.V. Adhikari, R.A. Kumar, Eur. J. Med. Chem. 45 (2010) 957.
[8] A.H. Kategaonkar, P.V. Shinde, A.H. Kategaonkar, S.K. Pasale, B.B. Shingate, M.S. Shingare, Eur. J. Med. Chem. 45 (2010) 3142.
[9] M.A. Matulenko, A.I. Meyers, J. Org. Chem. 61 (1996) 573.
[10] P. Magnus, D. Parry, T. Illiadis, S.A. Eisenbeis, R.A. Fairhuist, J. Chem. Soc., Chem. Commun. (1994) 1543.
[11] N. Ahmed, K.G. Brahmbhatt, S. Sabde, D. Mitra, I.P. Singh, K.K. Bhutani, Bioorg. Med. Chem. 18 (2010) 2872.
[12] S. M. Roopan, F. R. N. Khan, ARKIVOC, 2009, xiii, 161.
[13] S. Bairagi, A. Bhosale, M.N. Deodhar, E-J. Chemi. 6 (2009) 759.
[14] SHELXTL, Program for the Solution and Refinement of Crystal Structures, (version 6.14), Bruker AXS, Wisconsin, USA, 2000.
[15] G.M. Sheldrick, SHELX-97: Program for the Solution and refinement of Crystal Structures, University of Göttingen, Germany, 1997.
[16] (a) C.F. Macrae, I.J. Bruno, J.A. Chisholm, P.R. Edgington, P. McCabe, E. Pidcock, L. Rodriguez-Monge, R. Taylor, J. van de Streek, P.A. Wood, J. Appl. Cryst. 41 (2008) 466;
(b) L.J. Farrugia, J. Appl. Cryst. 30 (1997) 565;
(c) L.J. Barbour, Supramol. Chem. 1 (2001) 189.
[17] Heber, Dieter Archiv der Pharmazie (Weinheim, Germany) 320 (1987) 595.
[18] (a) M.A. Spackman, J.J. McKinnon, CrystEngComm 4 (2002) 378;
(b) J.J. McKinnon, F.P.A. Fabbiani, M.A. Spackman, Crystal Growth Des. 7 (2007) 755.